Geological Controls on Matrix Permeability of the Doig-Montney Hybrid Shale-Gas–Tight-Gas Reservoir, Northeastern British Columbia (NTS 093P)

G.R.L. Chalmers, **University of British Columbia, Vancouver, BC, gchalmer@eos.ubc.ca**

R.M. Bustin, **University of British Columbia, Vancouver, BC**

A.A.M. Bustin, **University of British Columbia, Vancouver, BC**

Chalmers, G.R.L., Bustin, R.M. and Bustin, A.A.M. (2012): Geological controls on matrix permeability of the Doig-Montney hybrid shale-gas–tight-gas reservoir, northeastern British Columbia (NTS 093P); *in* Geoscience BC Summary of Activities 2011, Geoscience BC, Report 2012-1, p. 87–96.

Introduction

Exploration and development of the hybrid shale-gas–tight-gas play of the Lower Triassic Montney Formation in northeastern British Columbia in recent years has led to attention being focused on the overlying Doig Formation, with the objective to coproduce the Doig and Montney plays. The Doig Formation has proven production from the Doig sandstone tight-gas play within the Groundbirch-field area (Walsh et al., 2006) and, currently, positive tests are reported from the Doig phosphate zone shale-gas play (Proust, 2010). The majority of production is associated with the middle Doig Formation and, to a lesser extent, with the upper Doig Formation within the Groundbirch area (D. Ross, personal communication). As very large gas-in-place estimates are common for shale-gas plays (i.e., 250 tcf for the Montney Formation; Adams, 2010), a better understanding of the geological controls on matrix permeability is needed. Fluid flow and the production rates of a shale-gas play are influenced by the matrix permeability of the reservoir and the length of the flow path, and hence, by the size of matrix blocks. Sedimentology has a large impact on the mineralogy, total organic carbon (TOC) content, fabric and texture of shale. The combination of these characteristics governs the pore-size distribution and the matrix permeability of the reservoir, which directly affects the productivity of the shale-gas play and development strategies.

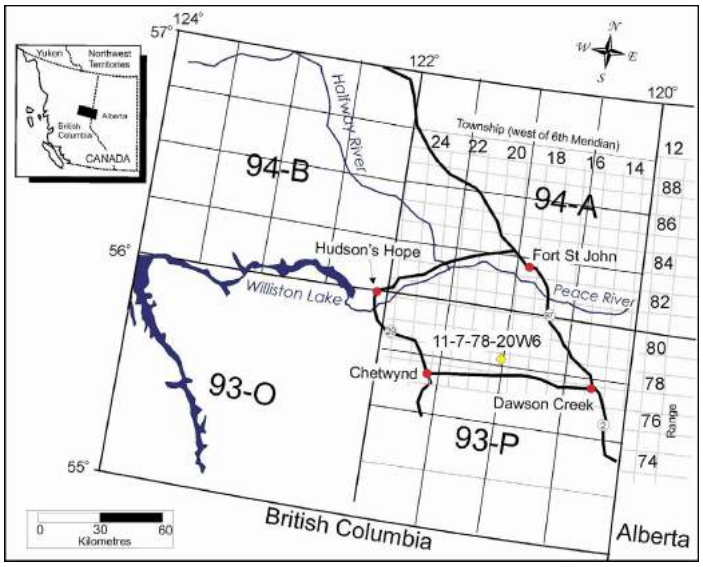

Figure 1. Index map showing the location of the 11-7-78-20W6 well sampled for this project (yellow diamond) and area cities and towns (red circles).

As part of this study to quantify and interpret the reservoir characteristics of gas-shale units in northeastern BC, a detailed study of the Montney–Doig interval in the productive Groundbirch area, south of Fort St. John, will be conducted. This preliminary report describes the results of high-resolution stratigraphic analyses of the mineralogy and pore system of strata in the 11-7-78-20W6 well (Figure 1). The objectives of this study are to

- determine the influence sedimentology has on the TOC-content distribution, the mineralogy, the porosity and the pore-size distribution;
- resolve the influence mineralogy has on the porosity and the pore-size distribution; and
- identify the controls on matrix permeability.

Geological Background

The Daiber Group within the Peace River plains area of northeastern BC consists of the Lower Triassic Montney and the Middle Triassic Doig formations (Figure 2). The Montney and Doig formations were deposited along a passive continental margin and consist of a westward-thickening, siliciclastic, prograding wedge (Edwards et al., 1994; Davies, 1997; Walsh et al., 2006; Dixon, 2009a, b); they represent the first and second of three transgressive-regres-

Keywords: *pulse-decay permeability, mineralogy, total organic carbon content, porosity and pore-size distribution*

sive (T-R) cycles, respectively, that deposited the Triassic strata in northeastern BC (Edwards et al., 1994). The depositional setting for the Montney and Doig formations is described as an open-shelf marine environment (Edwards et al., 1994). Paleogeographic reconstruction for Triassic sedimentation interprets a paleoshoreline that prograded during sea-level regressions to just east of Fort St. John and the BC-Alberta border (Kent, 1994). Throughout that period, shallow shelf mud covered the study area and deeper marine mud was deposited to the west of the study area.

In this study, the Montney and Doig formations are subdivided into units A to D (Figure 2) to simplify descriptions and comparison. The Montney Formation consists of variable amounts of interbedded shale, siltstone and sandstone. Dixon (2000) subdivided the Montney Formation within BC into the lower siltstone-sandstone and the upper shale members based on lithostratigraphy. The two members are separated by a basin-wide unconformity resulting from tectonic uplift of the basin margin (Dixon, 2009b) and are interpreted as the result of two higher-order T-R couplets (Uttings et al., 2005). The upper shale member of the Montney Formation (unit A in this study) is absent within Alberta and progressively becomes thicker (up to 159 m) to the west, towards the foothills of BC (Dixon, 2000).

Overlying the Montney Formation is the second T-R cycle, which deposited the Doig (units B to D of this study), Halfway (unit E) and Charlie Lake formations (Figure 2). The

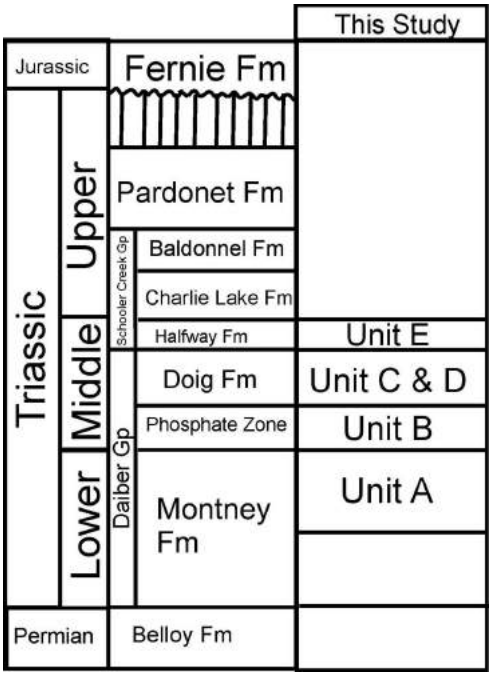

Figure 2. Stratigraphic columns for the Triassic strata within the Peace River plains area of northeastern British Columbia and the five units referred to within this study (modified from Davies, 1997). Abbreviations: Fm., Formation; Gp., Group.

Doig Formation is informally subdivided by Davies (1997) into three distinct lithological units: the lowermost phosphate zone (unit B); middle siltstone (unit C); and the upper regressive, coarsening-upward sequence (unit D). Thickness of the Doig Formation varies from 790 m, southwest of Fort St. John, to 80 m, toward the northeast, at the BC-Alberta border. Unit B is a highly radioactive unit, which consists of phosphatic nodules and granules within argillaceous siltstone, interbedded with calcareous siltstone and dark-grey shale (Riediger et al., 1990). The Doig Formation was deposited in a distal- to mid-shelf setting during a marine transgression. The middle Doig (unit C) is a medium to dark-grey argillaceous siltstone and shale unit deposited in a distal-shelf setting, which locally contains a shoreface sandstone up to 25 m thick (Evoy, 1998). This sandstone unit, interpreted as deltaic to shoreface sandstone, is part of the highstand-systems tract that deposited unit C (Harris and Bustin, 2000); highstand-systems tracts contain aggradational to progradational parasequence sets, which are bounded by a downlap surface and a sequence boundary. Unit D contains siltstone and fine sandstone, and the boundary with the overlying unit E lies between a muddier Doig sandstone and an overlying cleaner Halfway sandstone (Figure 2; Evoy, 1998). Unit D is interpreted as having been deposited in a proximal-shelf to lower-shoreface environment. The Doig Formation is overlain by the prograding beach-barrier sandstone of unit E (Figure 2).

Methods

To evaluate the reservoir characteristics of the Montney and Doig formations, sidewall cores and core plugs were collected from the 11-7-78-20W6 well. Samples were analyzed to determine the TOC content, T_{max}, organic geochemistry, mineralogy, porosity, pore-size distribution (PSD) and permeability. The TOC content, organic geochemistry and T_{max} values were collected using a Rock Eval™ II apparatus with a TOC module.

A normal-focus cobalt X-ray tube was used on a Siemens D5000 diffractometer generated at 40 kV and 40 mA for X-ray diffraction analysis. Crushed samples (<250 µm) were mixed with ethanol, hand-ground in a mortar and pestle and smear-mounted on glass slides. The mineral composition was quantified by Rietveld analysis (Rietveld, 1967) using Bruker AXS TOPAS V3.0 software.

Porosity was calculated from the bulk density and the skeletal density. Mercury immersion determined the bulk density of a sample. Skeletal density was obtained by helium pycnometry on oven-dried samples (i.e., $S_w = 0$) with a grain size between 0.841 mm (sieve size of 20 mesh) and 0.595 mm (sieve size of 30 mesh). Pore-size distribution, pore area and porosity were measured by a Micromeritics AutoPore porosimeter on crushed samples (sieve size of

20–30 mesh). To measure the pore-size distribution, cylindrical pore geometry is assumed and the pore radius is calculated from the applied pressure using the Washburn equation (Washburn, 1921). The porosimetry-derived porosity is the ratio between the total intrusion volume of the sample and the bulk volume of the sample. As a requirement of the analytical procedure of degassing and evacuating samples prior to analysis, the latter were oven dried at 110°C, which results in the water saturation being zero (S_w = 0). The pore-size detection limit of this analysis is 3 nm (approximate boundary between mesopore and micropore[1]), with the pore size being calculated from the Washburn equation. Therefore the porosimetry-derived porosity results do not consider water saturation or the microporosity of the sample.

Permeability was determined by a pulse-decay permeameter using helium on core plugs and sidewall cores 2.5 cm in diameter and length. Permeability was measured with an effective stress of 22.8 MPa (3300 psi, in situ reservoir pressure).

Results

Mineralogy

The Doig and Montney formations are dominated by carbonate (calcite and dolomite), quartz and feldspar (albite and microcline) with minor quantities of illite, pyrite and apatite (Figure 3; Bustin et al., 2011, Figure 6), although illite content can be locally important. In the case of well 11-7-78-20W6, the quartz content ranges between 13 and 74%, with an average of 31%, and increases from unit B to the base of unit E (Figure 3). Carbonate content averages 23% and ranges between 2 and 51%, whereas that of dolo-

[1] Micropores (<2 nm), mesopores (2–50 nm) and macropores (>50 nm) are defined by the physical gas-adsorption characteristics of microporous and mesoporous media.

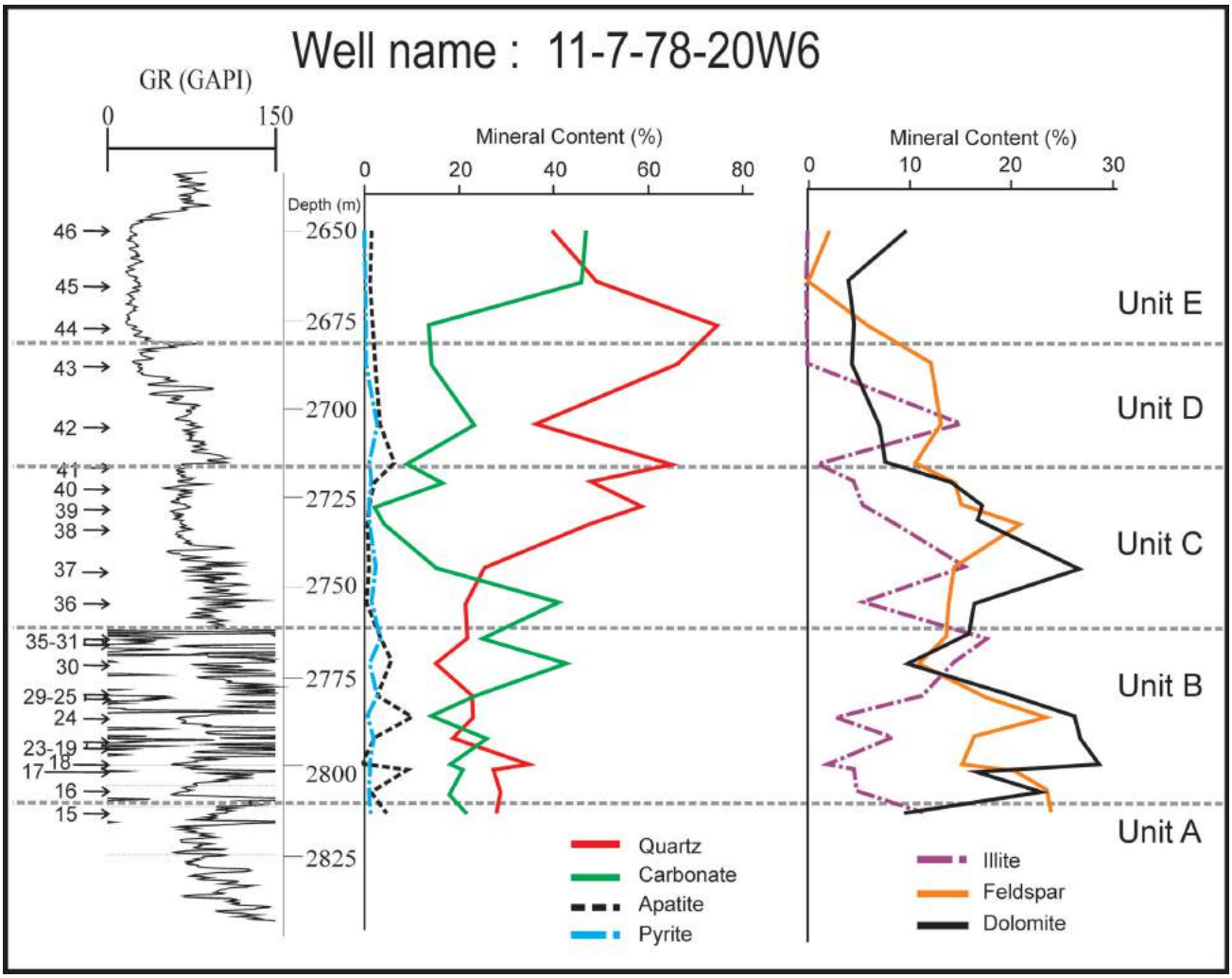

Figure 3. Mineralogical trends for the 11-7-78-20W6 well in northeastern British Columbia. Carbonate includes calcite and ankerite, although calcite dominates (i.e., ankerite averages 1.4%, and ranges between 0 and 7.2%). GR represents the geophysical gamma-log profile measured in American Petroleum Institute units (GAPI). Sample locations are shown on the left side of the diagram.

mite averages 17% and varies between 4 and 34%. The feldspar content averages 15% and ranges between 0 and 24%. The basal portion of unit B is carbonate- and/or dolomite-rich, which content decreases from the upper portion of unit C toward unit E, mirroring the quartz trends (Figure 3). The average illite content is 9% and ranges between 0 and 20%; higher illite contents are found within the upper portion of unit B and the lower (finer-grained) portions of units C and D. Pyrite averages 1.8% and varies between 1 and 5%. The Pearson product-moment correlation shows that the strongest relationships occur between total carbonate (calcite, ankerite and dolomite) and quartz (r = -0.71), illite and pyrite (r = 0.74), and between quartz+feldspar and carbonate (calcite+ankerite, r = -0.62).

Porosity

Porosity was determined by helium pycnometry and mercury porosimetry, with the former measuring pore sizes greater than the kinetic diameter of helium (0.26 nm) and the latter restricted to measuring pore sizes greater than 3 nm. Although the 3 nm boundary is derived from the Washburn equation and the assumption that all pores are cylindrical may not be correct, the relative difference between the two methods does indicate that pores present within some samples are undetectable using porosimetry. Therefore, any differences seen in the results obtained from these two methods (i.e., pycnometry-derived porosity and porosimetry-derived porosity) are considered an indication that there are pores within the size range of 0.26 to 3 nm (microporosity and fine mesoporosity). Pycnometry-derived porosity for the 11-7-78-20W6 well varies between 1.6 and 6.7%, with an average of 4.2%, and porosimetry-derived porosity varies between 1.9% and 6.5%, with an average of 3% (Figure 4). The two porosity profiles show a large difference within unit B and within unit D (Figure 4), indicating an increase in the fine meso- and microporosity (i.e., 0.26–3 nm) within these intervals. Above average porosity occurs within the coarser sections of the Doig Formation—at the base of unit B, and at the top of units C and D. Unit E and finer-grained intervals of units B, C and D have below-average porosity (Figure 4). Positive Pearson product-moment correlation coefficients exist between porosity and quartz content (r = 0.58), as well as between porosity and quartz+feldspar content (r = 0.59). Negative correlation coefficients exist between porosity and carbonate content (r = -0.71), and between porosity and total carbonate content (r = -0.55).

Pore-Size Distribution

Pore-size distribution (PSD) is illustrated by pore volume and by pore area for well 11-7-78-20W6 (Figures 5, 6). Unit B samples contain a high volume of pores within the 10 000–100 000 nm macropore size range and within the 3–50 nm mesopore size range. Variations in the proportion of

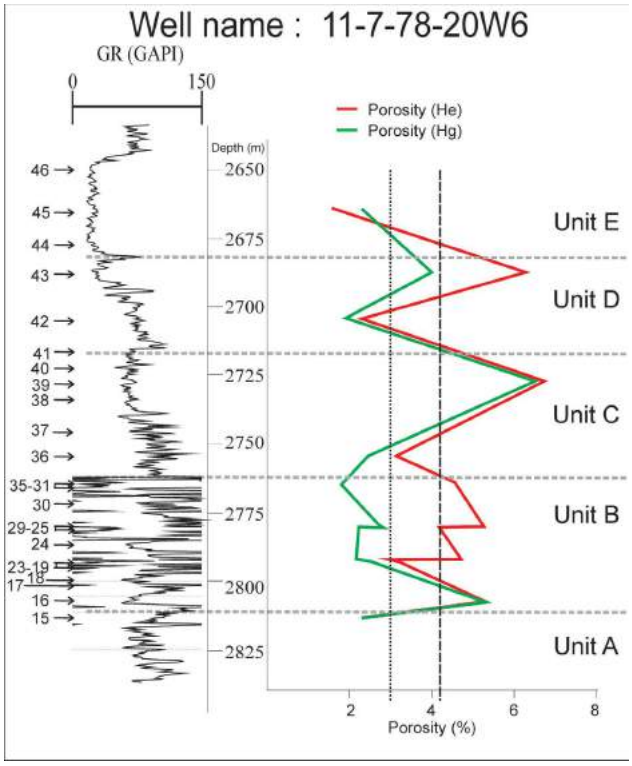

Figure 4. Pycnometry- and porosimetry-derived porosity profiles of the 11-7-78-20W6 well. The dotted line represents the average porosimetry-derived porosity and the dashed line represents the average pycnometry-derived porosity. Samples are oven dried to compare between methods as moist samples cannot be used for porosimetry (i.e., $S_w = 0$). GR represents the geophysical gamma-log profile measured in American Petroleum Institute units (GAPI). Sample locations are shown on the left side of the diagram.

macro- and mesopores exist between samples; those from units C, D and E (Figure 5a, b) have smaller proportions of mesopores compared to those from unit B (Figure 5c, d). Siltstone and very fine sandstone samples (e.g., sample 11-7-33; Figure 5c) from unit B also contain lower proportions of mesopores compared to finer-grained samples (e.g., sample 11-7-27; Figure 5c). Macropores, particularly in the 10 000–100 000 nm size fraction, do not significantly contribute to the pore area in comparison to mesopores and fine macropores (Figure 6).

Organic Geochemistry

The TOC content for the 11-7-78-20W6 well varies from 0.5 to over 7 wt %, with an average content of 3.2% (Figure 7). Samples from unit E and the top of unit D yielded TOC values below the detection limit of the Rock Eval™ apparatus (<0.5 wt %) and are therefore not included on the profile. Unit A (sample 11-7-15), the upper two-thirds of unit B, and unit C (sample 11-7-37) all register above average TOC-content values, which show high variability throughout the profile, the largest variation occurring in unit B (i.e., samples 11-7-25 to 11-7-29). A positive corre-

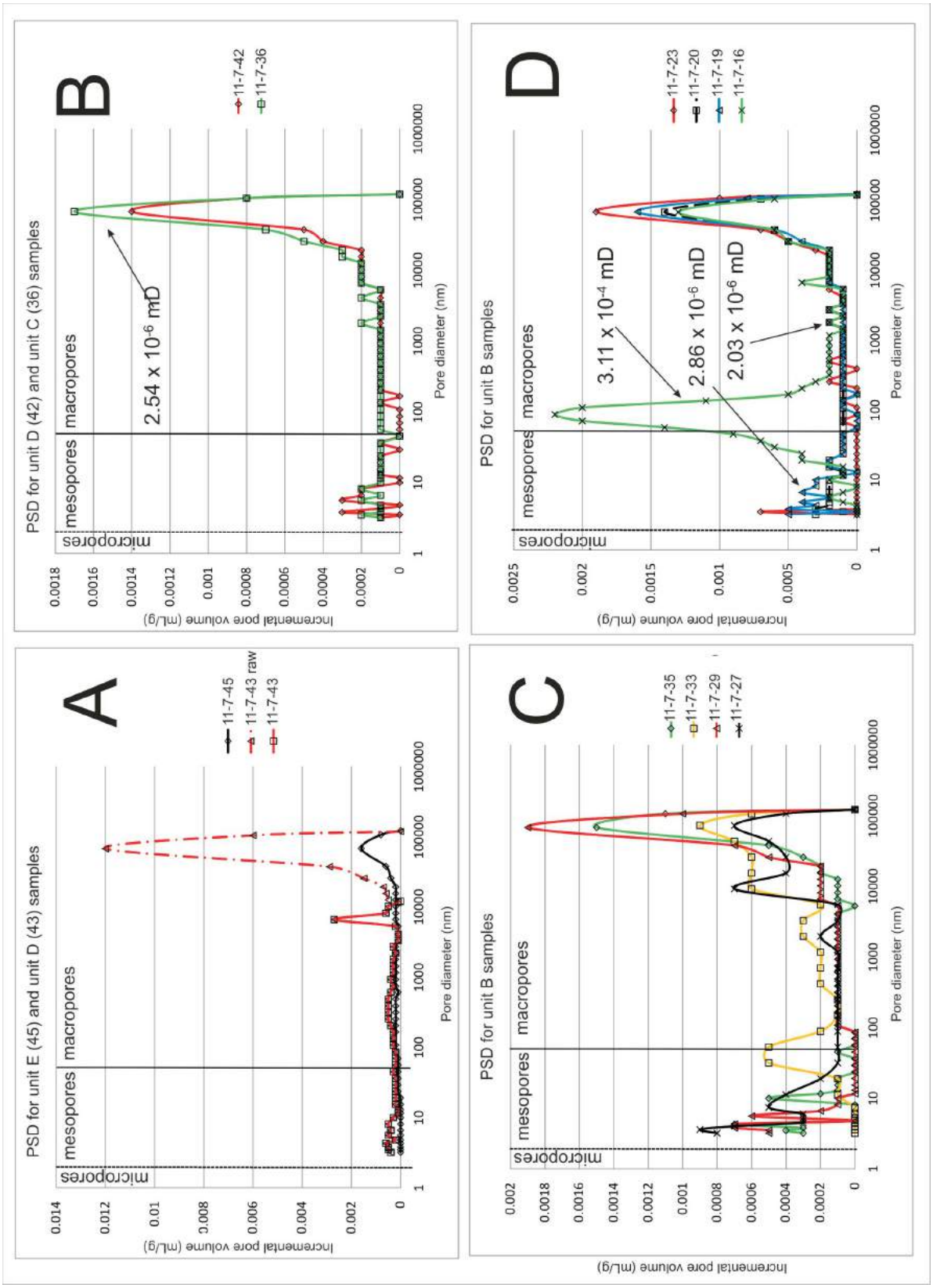

Figure 5. Pore-size distribution (PSD) for the 11-7-78-20W6 well, expressed using the incremental pore volume (mL/g). The dashed line represents the boundary between micro- and mesopores (2 nm) and the solid line demarcates the boundary between meso- and macropores (50 nm). Helium pulse-decay permeability (in mD) is also shown for some samples. Coarser-grained samples from units C, D and E show less mesopore volumes (Figure 5a, b) compared to samples from unit B (Figure 5c, d). Samples were crushed to a sieve size of 20–30 mesh. Sample locations can be found on Figure 4.

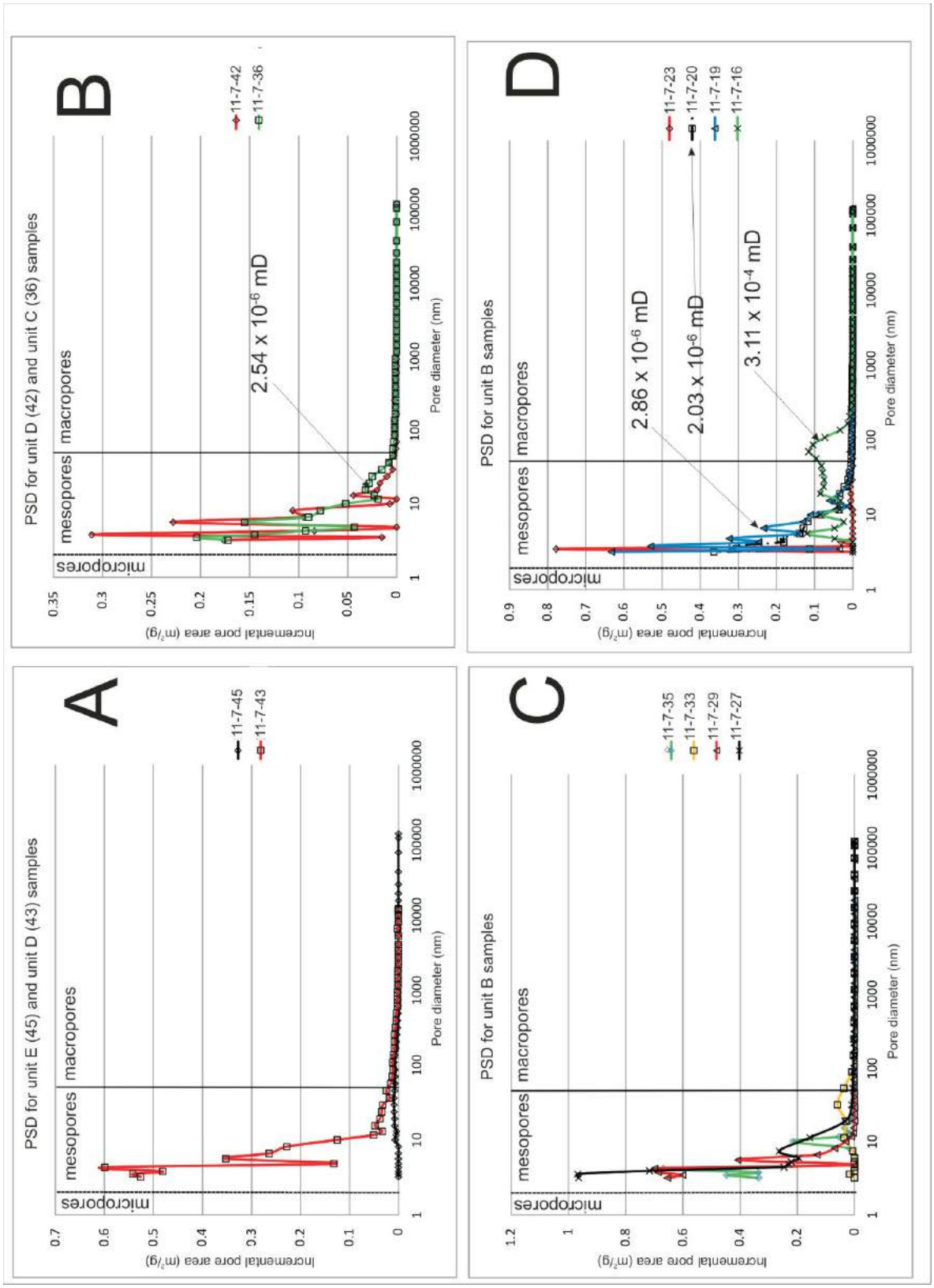

Figure 6. Pore-size distribution (PSD) for the 11-7-78-20W6 well, expressed using the incremental pore area (m^2/g). The dashed line represents the boundary between micro- and mesopores (2 nm) and the solid line represents the boundary between meso- and macropores (50 nm). Helium pulse-decay permeability (in mD) is also shown for some samples. Greater pore area is found in the finer-grained unit B samples (Figure 6c, d) compared to the coarser-grained units C to E samples (Figure 6a, b). Samples were crushed to a sieve size of 20–30 mesh. Sample locations can be found on Figure 4.

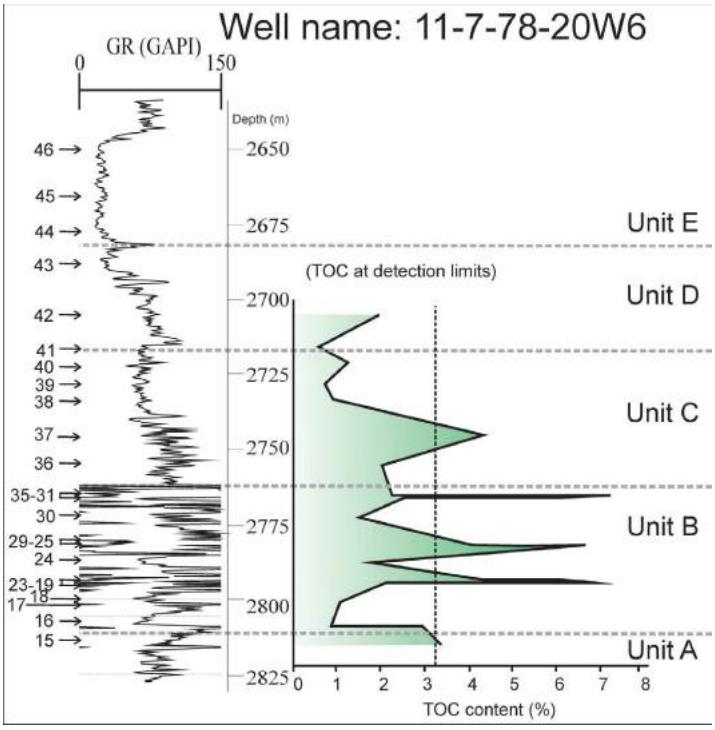

Figure 7. Total organic content (TOC) profile for the 11-7-78-20W well. TOC-content values were below the detection limit of the Rock Eval™ apparatus for samples collected within the Halfway Formation (unit E) and lower Doig member (unit D) and are therefore not included. The dashed line represents the average TOC content of 3.2 wt %. GR represents the geophysical gamma-log profile measured in American Petroleum Institute units (GAPI). Sample locations are shown on the left side of the diagram.

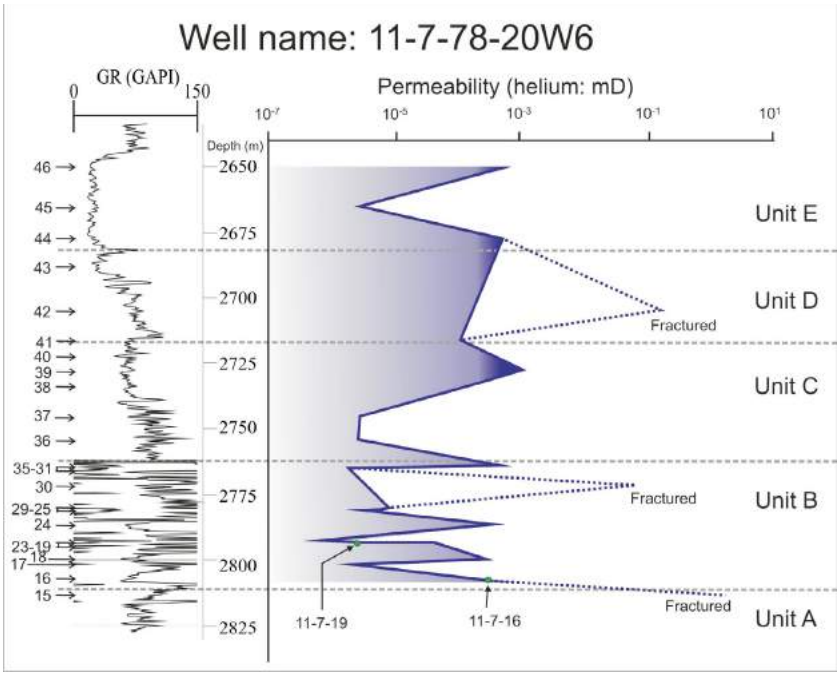

Figure 8. Downhole permeability trend for the 11-7-78-20W6 well, including the matrix permeability (solid line) and fracture permeabilities (dashed lines). The low frequency alternation within units C and D compared to unit B may be an artefact of their lower sampling resolution. GR represents the geophysical gamma-log profile measured in American Petroleum Institute units (GAPI). Sample locations are shown on the left side of the diagram.

lation exists between TOC and pyrite (r = 0.68) whereas a negative trend exists between quartz and TOC content (r = -0.56).

The hydrogen index (HI) for the 11-7-78-20W6 well averages 20 mg HC/g TOC, and ranges between 1 and 76 mg HC/g TOC. The oxygen index (OI) averages 34 mg CO_2/g TOC, and ranges between 5 and 172 mg CO_2/g TOC. The average T_{max} value is 457°C, and ranges between 443 and 478°C, placing the reservoirs within the gas window.

Pulse-Decay Permeability

The matrix permeability ranges between 10^{-4} and 10^{-7} mD (Figure 8); it also varies by two orders of magnitude between samples 11-7-16 and 11-7-19 (Figure 8), in part due to the difference in their PSD (see discussion for details). The higher matrix permeabilities in the 11-7-78-20W6 well are located in the top of unit C and scattered throughout unit B (solid line, Figure 8). The high alternation of permeability values within unit B may be due to the lithological and/or mineralogical changes and the lack of similar trends within units C, D and E could be an artefact of their lower sampling resolution compared to unit B. Samples that contain fractures (dashed lines, Figure 8) exhibit permeabilities that are four to five orders of magnitude greater than the lower permeabilities.

Discussion

Controls on Mineralogy

Unit B is carbonate and/or clay-rich and quartz-poor with units C and D being quartz-rich and carbonate and/or clay-poor (well 11-7-78-20W6; Figure 3). The Montney Formation (unit A) is carbonate-poor and quartz-rich compared to the Doig phosphate zone (unit B). The contrasting mineralogical character of the quartz-rich units C and D and carbonate-rich unit B in well 11-7-78-20W6 indicates a change in the sedimentary environment, accommodation space and/or tectonic activity within the study area as the depositional conditions shifted from carbonate deposition to clastic deposition. A greater influx of clastic rocks in the upper Doig Formation is either due to increasing tectonic activity or to a reduction in accommodation space (shoreline progradation) as a sea-level regression progressed. Clay deposition occurred when quartz and feldspar influx was low and pyrite deposition, high. The higher pyrite content (i.e., greater than 4%) indicates that the depositional conditions were dysoxic[2] to anoxic during periods of clay deposition. A negative relationship between quartz+feldspar and total carbonate contents indicates that during periods of quartz- and feldspar-rich detritus influx, carbonate and dolomite deposition was low, whereas when influx of quartz and feldspar diminished, carbonate production relatively increased. Carbonate and clay sedimentation does not occur simultaneously (i.e., during low influx of quartz and feldspar), as indicated by the strong negative correlation between illite and carbonate. The deposition of the quartz, feldspar and clay minerals may be a result of turbiditic events, with fining-upward sequences ending in clay deposition; it therefore appears that carbonate deposition was restricted to the quiescent, non-turbiditic periods.

Controls on Porosity and Pore-Size Distribution

An increase in the difference between the pycnometry- and porosimetry-derived porosity occurs within unit B, indicating an increase in the fine meso- and microporosity (<3 nm) in the more carbonate/clay- and TOC-rich unit B compared to the other units (Figure 4).

The negative correlation between porosity and carbonate content could be an indication that porosity is low due to carbonate cementation, to recrystallization or to micritic mud deposition. Carbonate cementation of the pore network may be responsible for the porosity reduction within unit E (sample 11-7-45) with a high carbonate content and low porosity (Figure 4). The positive correlation between porosity and the quartz+feldspar content is indicative of an enhancement in the intergranular porosity. Higher porosity intervals within unit B are due to the localized increase in quartz content in an otherwise clay- and/or carbonate-rich unit.

Siltstone samples have a high volume of macropores and large mesopores (20–50 nm), high quartz content and low TOC and clay contents (e.g., sample 11-7-42 in unit D or sample 11-7-16 in unit B; Figures 3, 5, 6) compared with other samples characterized by low quartz, high clay and high TOC contents (e.g., samples 11-7-27 and 11-7-29 of unit B; Figures 3, 5, 6). Clay- and TOC-rich samples contain a higher proportion of mesopores, which results in a higher proportion of surface areas compared with siltstone samples; surface area provides gas storage in the sorbed state within the reservoir (Chalmers and Bustin, 2008).

Controls on the Distribution of the TOC Contents

Unit B contains the highest TOC contents, the lowest quartz contents and the highest contents of carbonate and/or clay compared to the other units. This observation is highlighted by the negative correlation between quartz and TOC contents. Higher TOC contents (Figure 7) in unit B are likely due to the increase in accommodation space, an increase in bottom-water anoxia, organic productivity and a reduction in clastic-rock influx. The positive correlation between TOC and pyrite indicates the bottom waters were anoxic to

[2] *having a very low oxygen content (i.e., between anoxic and hypoxic)*

euxinic during the deposition of unit B. A large variation in the TOC content can occur between closely-spaced samples (i.e., 20 cm for samples 11-7-31 to -35), which may be an indication that changes were occurring in the depositional environment or that turbiditic or storm events affected the preservation and accumulation of the organic matter. Low HI and OI values indicate that either the kerogen has experienced a high degree of hydrocarbon generation or that it originally came from oxidized plant material. The Montney and Doig formations are thermally mature to overmature (Riediger et al., 1990).

Controls on Matrix Permeability

The PSD, which controls the matrix permeability of the Doig and Montney reservoirs, was compared between samples that differed in matrix permeability by two orders of magnitude (Figure 5d, samples 11-7-16 and 11-7-19). Sample 11-7-16, which is characterized by a higher permeability, has a greater proportion of pores at the mesopore–macropore boundary compared with sample 11-7-19, which contains a greater volume of pores at the micropore–mesopore boundary. Both high- and low-permeability samples have bimodal pore-size distribution. The degree of separation between the two populations of pore sizes of the low-permeability samples (e.g., sample 11-7-19) is four orders of magnitude greater than that of the higher permeability samples (e.g., sample 11-7-16), whose degree of separation of only three orders of magnitude suggests a greater degree of communication within the matrix. The contrasting PSD are due to the differences between the mineralogy and TOC contents. The difference between the high (10^{-4} mD) and low ($<10^{-6}$ mD) permeabilities of samples from well 11-7-78-20W6 (Figure 8) is due, in part, to the mineralogy; as shown on Figure 9, carbonate-rich samples have lower permeability than quartz-rich samples. Carbonate cementation during diagenesis and/or deposition of fine-grained micritic mud reduces both the porosity and permeability of the Doig and Montney formations.

Conclusions

Ongoing evaluation of the Doig and Montney reservoirs within the Groundbirch area of northeastern BC includes characterizing the mineralogy, porosity, pore-size distribution, organic geochemistry and matrix permeability. Downhole profiles illustrate the small-scaled heterogeneity in the mineralogy, TOC content and porosity. The finer-grained, high TOC-content, carbonate- and/or clay-rich intervals have lower permeability than the coarser-grained, lower TOC-content, carbonate- and/or clay-poor and quartz-rich intervals. Higher TOC contents in finer-grained intervals mean larger volumes of sorbed gas would be stored but its delivery to the wellbore would be slower, due to the lower permeability of these intervals compared with the higher permeability of the quartz-rich intervals.

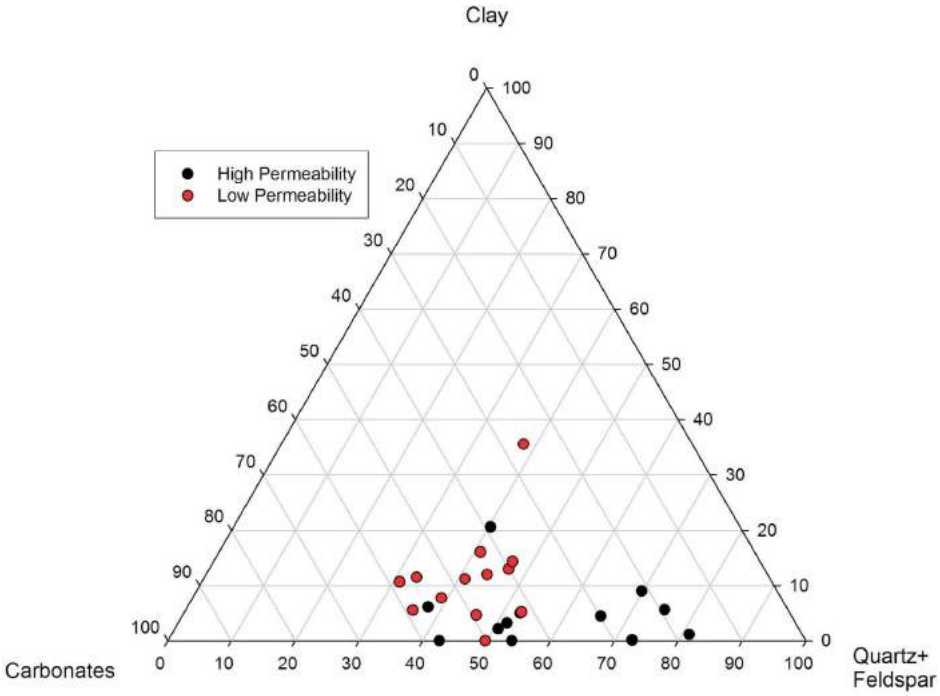

Figure 9. Mineralogical ternary diagram showing the difference between high and low matrix permeabilities.

Future Work

Data is currently being collected and interpreted from three more wells within the Groundbirch area. Inorganic petrology is to be conducted to examine the relationships between fabric, mineralogy, porosity and permeability. Organic petrology will also be performed to gain an understanding of the controls on organic sedimentation (i.e., terrestrial- versus marine-sourced organic materials).

Acknowledgments

The authors would like to thank Geoscience BC for its financial support of this ongoing research. They would also like to thank D. Ross who reviewed an earlier version of this manuscript.

References

Adams, C. (2010): Shale gas activity in British Columbia: Exploration and Development of BC's shale gas areas (abstract); BC Ministry of Energy and Mines, 4th Annual Unconventional Gas Technical Forum, April 8–9, 2010, Victoria, BC, URL <http://www.em.gov.bc.ca/OG/oilandgas/petroleumgeology/UnconventionalGas/Documents/C%20Adams.pdf> [October, 2011].

Bustin, R.M., Chalmers, G., Bustin, A.A.M. (2011): Quantification of the gas-in-place and flow characteristics of tight gas-charged rocks and gas-shale potential in British Columbia; *in* Geoscience BC Summary of Activities 2010, Geoscience BC, Report 2011-1, p. 201–208, URL <http://www.geosciencebc.com?i?pdf?SummaryofActivities2010/SoA2010_Bustin_etal.pdf> [October, 2011].

Chalmers, G.R.L. and Bustin, R.M. (2008): Lower Cretaceous gas shales in northeastern British Columbia, Part I: geological controls on methane sorption capacity; Bulletin of Canadian Petroleum Geology, v. 56, p. 1–21.

Davies, G.R. (1997): The Triassic of the western Canadian sedimentary basin: Tectonic and stratigraphic framework, palaeogeography, palaeoclimate and biota; Bulletin of Canadian Petroleum Geology, v. 45, p. 434–460.

Dixon, J. (2000): Regional lithostratigraphic units in the Triassic Montney Formation of western Canada; Bulletin of Canadian Petroleum Geology, v. 48, p. 80–83.

Dixon, J. (2009a): The Lower Triassic Shale member of the Montney Formation in the subsurface of northeast British Columbia; Geological Survey of Canada, Open File 6274, 9 p.

Dixon, J. (2009b): Triassic stratigraphy in the subsurface of the plains area of Dawson Creek (93P) and Charlie Lake map areas (94A), northeast British Columbia; Geological Survey of Canada, Bulletin 595, 78 p.

Edwards, D.E., Barclay, J.E., Gibson, D.W., Kvill, G.E. and Halton, E. (1994): Triassic Strata of the Western Canada Sedimentary Basin; *in* Geological Atlas of the Western Canada Sedimentary Basin, G.D. Mossop and I. Shetsen (comp.), Canadian Society of Petroleum Geologists and Alberta Research Council, Special Report 4, URL <http://www.ags.gov.ab.ca/publications/wcsb_atlas/atlas.html> [August, 2011].

Evoy, R.W. (1998): Reservoir sedimentology of the Doig Formation, Buick Creek Field, Northeastern British Columbia; *in* Oil and Gas Pools of the Western Canada Sedimentary Basin, J.R. Hogg (ed.), Canadian Society of Petroleum Geologists, Canada, Special Publication S-51, p. 127–135.

Harris, R.G. and Bustin, R.M. (2000): Diagenesis, reservoir quality and production trends of Doig Formation sand bodies in the Peace River of western Canada; Bulletin of Canadian Petroleum Geology, v. 48, no. 4, p. 339–359.

International Union of Pure and Applied Chemistry, (1997): Compendium of Chemical Terminology (2nd edition); A.D. McNaughton and A. Wilkinson (comp.), Blackwell Scientific Publications, Oxford, doi: 10.1351/goldbook.M03906, URL <http://goldbook.iupac.org/M03906.html> [November 2011].

Kent, D.M. (1994): Paleogeographic evolution of the cratonic platform – Cambrian to Triassic; *in* Geological Atlas of the Western Canada Sedimentary Basin, G.D. Mossop and I. Shetsen (comp.), Canadian Society of Petroleum Geologists and Alberta Research Council, Special Report 4, URL <http://www.ags.gov.ab.ca/publications/wcsb_atlas/atlas.html> [August 4, 2010].

Proust, J. (2010): Canada Energy Partners announces successful horizontal Montney test; Canada Energy Partners, press release, July 6, 2010, URL <http://www.canadaenergypartners.com/news/2010/index.php?&content_id=107> [October 2011].

Riediger, C.L., Brooks, P.W., Fowler, M.G. and Snowdon, L.R. (1990): Lower and Middle Triassic source rocks, thermal maturation, and oil-source rock correlations in the Peace River embayment area, Alberta and British Columbia; Bulletin of Canadian Petroleum Geology, v. 38A, p. 218–235.

Utting, J., MacNaughton, R.B., Zonneveld, J.P. and Fallas, K.M. (2005): Palynostratigraphy, lithostratigraphy and thermal maturity of the Lower Triassic Toad and Grayling, and Montney formations of western Canada, and comparisons with coeval rocks of the Sverdrup basin, Nunavut; Bulletin of Canadian Petroleum Geology, v. 53, p. 5–24.

Walsh, W., Adams, C., Kerr, B. and Korol, J. (2006): Regional "shale gas" potential of the Triassic Doig and Montney formations, northeastern British Columbia; BC Ministry of Energy and Mines, Petroleum Geology Open File 2006-2.

Washburn, E.W. (1921): Note on a method of determining the distribution of pore sizes in a porous material; Proceeding of the National Academy of Sciences of the United States of America, v. 7, p. 115–116.